THERMAL CONDUCTIVITY AND DIELECTRIC PROPERTIES OF POLYPROPYLENE-BASED HYBRID COMPOUNDS CONTAINING MULTIWALLED CARBON NANOTUBES

P. Russo[1], A. Patti[2],*, C. Petrarca[3], S. Acierno[4]

[1]Institute for Polymers, Composites and Biomaterials, National Research Council, Via Campi Flegrei 34, Pozzuoli, Naples, 80078, Italy
[2]Department of Chemical, Materials and Industrial Production Engineering, University of Naples Federico II, Piazzale Tecchio 80, Naples, 80125,Italy
[3]Department of Electrical Engineering and Information Technology, University of Naples Federico II, Via Claudio 21, Naples, 80125,Italy
[4]Department of Engineering, University of Sannio, Piazza Roma 21, Benevento, 82100, Italy

Correspondence to: Antonella Patti (E-mail: *antonella.patti@unina.it*)

ABSTRACT

In this paper we explore the possibility to develop composites with improved thermal conductivity and electrically insulating properties. The strategy adopted is to combine a thermal and electrical conductive filler (Multi Walled Carbon NanoTubes) with secondary dielectric (but thermally conductive) fillers. To this end particles with different composition, sizes and shape were used as secondary fillers and the composites, prepared by melt compounding, are characterized in terms of thermal and dielectric properties. Results show that, in ternary formulations, an increase of thermal conductivity is always verified for all kind of secondary particles. Analogously, increments in electrical conductivity are observed for ternary compounds containing larger size secondary fillers, while a significant reduction is achieved with the addition of smaller ones. This behavior is explained in terms of mutual distribution of the fillers and is consistent with direct (scanning electron microscopy) and indirect (rheological) observations.

Keywords:

Thermal properties, Dielectric Properties, Polyolefins, Nanotubes, Graphene and Fullerenes

INTRODUCTION

In recent years, the addition of two or more fillers, having different nature, geometry and/or length scale, into a polymer matrix has gained an increasing attention as it allows to meet very specific engineering requirements [1]. These materials, best defined as “hybrid composites” or simply as “hybrids”, combine intrinsic properties of each component and may offer superior performances with respect to that of the individual elements. Leong et al. [2] studied the mechanical and thermal properties of hybrid polypropylene (PP) composites with two main types of mineral fillers—calcium carbonate ($CaCO_3$) and Talc, verifying a synergistic hybridization effect in flexural and impact strength when PP/CaCO3/Talc weight ratio was 70/15/15. Salkhord et al.[3] analyzed the influence of hybrid fillers, as modified silicate and nano-calcium carbonate (nano-CaCO3), on mechanical properties of the nitrile rubber (NBR). The dual-filler phase nanocomposites showed higher performance in comparison with single-filler phase nanocomposites. The efficiency of combined boron nitride (BN) and zinc oxide (ZnO) particles in reducing wear rate and improving thermal conductivity of the polytetrafluoroethylene (PTFE) composites, was demostated by Luan at al. [4]. Hybrid PTFE composites displayed a higher thermal conductivity, much smoother worn surfaces and slighter ploughing than those with individual filler at the same content.

In general, the behavior of hybrid composites is profoundly influenced by the formation of a co-supporting network, which is influenced by the mutual distribution and nature of the fillers. In this regard, depending on the contents, the inclusion of fillers having different sizes may promote the development favorable mutual packing [5]. Pak et al. [6] detected synergic improvements in thermal conductivity of polyphenylene sulfide based composites realized with the addition of BN and MWCNTs surface modified with hydrogen peroxide and acid treatments. The good results were attributed to the generation of three-dimensional thermal transfer paths, between fillers and surface-modified MWCNTs, that strongly affect the interfacial interaction and thermal resistance. Palza et al. [7] evaluated the effect of addition of nanoparticles with different geometry (montmorillonite clay, copper nanoparticles, and spherical silica) on electrical conductivity of PP composites containing up to 5.5 vol. % of CNTs. They found that for spherical silica particles the reduction of the free volume for CNTs dispersion leads to an apparent increase of their effective concentration for electric conductivity while, in case of layered clays, their higher aspect ratio could hinder interconnections between CNTs, by acting as a wall between them, and damage the conductive pathways. More recently, Tsekmes et al. [8] found that the addition of a little amount of nanofillers in epoxy microcomposites with high filler loading improves both thermal and electrical conductivities of the hybrids. In particular, 0.6 vol. % of nanosized hexagonal BN, added to an epoxy microcomposite reinforced with 60 wt% of silica microparticles, increases the thermal conductivity by 30%, the direct current (DC) breakdown strength by 50%, and the alternating current (AC) breakdown strength by 65%. The enhanced performances were discussed in terms of increased interaction between the polymer matrix and the microfillers due to the insertion of the nanoparticles.

Among potential applications of hybrid systems, it is worth to mention the field of electronic packaging and miniature devices, automotive or heat exchangers in which the heat removal

has become a crucial issue and economic lightweight solutions are needed. In this regard, remarkable benefits can be achieved by including two mixed highly thermally conductive fillers in polymer matrices with opportune geometries. Dang et al. [9] combined micrometric whiskers and spheres of AlN, in various volume ratios, in epoxy and polyvinylidene fluoride (PVDF) matrices. The effect of aluminum oxide (Al_2O_3) and AlN with large and small size is reported in [10] while microparticles of graphite and silicon carbide (SiC) were considered in epoxy resins for the ability in dispersion and low cost of the former and the high temperature and high power applications of the latter [11]. Furthermore, BN flakes and tetrapod-shaped zinc oxide (T-ZnO) whiskers were employed to obtain thermally conductive but electrically insulating phenolic formaldehyde resin [12] and nano-graphene/micro-graphite were added in epoxy resins at different overall concentration [13].
In view of the recent research attention to carbon nanotubes, given their intrinsic high thermal conductivity (3000 W/mk), as fillers in the realization of thermally conductive plastics [14], we have, in a recent work, verified the improvements of heat conduction in polypropylene by adding CNTs [15]. Nevertheless, the inherently high electrical conductivity of the above nanoparticles limits the use in applications requiring thermally conductive and contemporary electrically insulating materials. In the light of literature on hybrids [16], in the present work we explore the possibility to overcame this limitation through the simultaneous inclusion of a carbonaceous filler and a secondary electrically inert particle with opportune thermal conductivity and investigate the possible relationship between secondary fillers' size effect on fillers dispersion and corresponding thermal and electrical conductivities of respective compounds.
In this framework, the aim of this study is to develop carbon-based thermally-conductive composites with low electrical conductivity. To reach this purpose, we propose polypropylene-based ternary formulations, combining carbon nanotubes (a thermal and electrical conductive filler) with additional thermally conductive, but electrically insulating, particles having different sizes and shape. By considering their previous applications in fields of thermally conductive composites [17-21], we have chosen ZnO, $CaCO_3$, BN, and talc as secondary fillers. The compounds are prepared by melt mixing and mainly characterized in terms of thermal and dielectric/electrical performances. Results, interpreted in terms of filler sizes and mutual dispersion, are supported by morphological direct observations through scanning electron microscopy and indirect inspections through dynamic rheological measurements.

EXPERIMENTAL

Materials

The matrix used in this study is a commercial polypropylene resin (Monsten MA524, M_n=32,400 g/mol; M_w=250,084 g/mol, melt flow index 24.0 g/10min at 230°C, 2.16 kg) supplied by UNIPETROL RPA.
Non-functionalized multi-wall carbon nanotubes, (MWCNT, Nanocyl NC3150) with average length < 1 μm and average outer diameter < 9.5 nm were used as the primary filler. Additional particles as specified in Table 1 (purchased from Sigma Aldrich Co. LLC., Milan, Italy) were used

as secondary filler in quantities corresponding to 10 vol. % and combined with 1.5 vol. % of MWCNT for the preparation of ternary systems.

Composites preparation

The composites were prepared using an internal mixer (Brabender Plastograph EC- Brabender GmbH & Co. KG, Germany) operated at 190°C, applying a screw speed of 60 rpm, and filling the mixing chamber with 40 cm^3 of material. During the mixing, the torque evolution was recorded in order to gain qualitative information about the system processability.
The as-received polypropylene pellets were introduced into the mixing chamber and processed for 2 minutes until a complete melting (evidenced by the achievement of a constant torque value). Afterwards, the fillers were added to the molten PP and the mixing was continued for further 5 minutes. With this procedure binary systems (PP/MWCNT) containing 1.5 vol. % of nanotubes and ternary systems (PP/MWCNT/X, with X representing the secondary filler) containing 1.5 vol. % of MWCNT and 10 vol. % of secondary filler were produced. The actual filler contents were verified by thermogravimetric analysis that always confirmed an excellent agreement between the effective and the nominal percentages in weight.

Characterization techniques

Thermal analyses were conducted by using Differential Scanning Calorimetry (DSC model Q20, from TA Instrument) on samples of about 10 mg. The enthalpy of fusion (ΔH_f) was measured during the second heating scan, at a heating rate of 10°C/min, and the degree of crystallinity (x_c) was calculated as:

$$x_c = \frac{\Delta H_f}{\Delta H_f^0 (1-\phi)} \cdot 100 \qquad (1)$$

where $(1-\phi)$ is the weight fraction of polymer within the composite and ΔH_f^0 is the theoretical enthalpy of fusion for a 100% crystalline polypropylene, taken to be 209 J/g [23].
Disc-shaped specimens, with a diameter of 50 mm and a thickness of 1.4 mm, were prepared by compression moulding and used for thermal and electrical characterization. The thickness was obtained by taking, for each sample, 5 measurements at different positions and calculating the average value. Steady-state thermal conductivity measurements were performed in through-plane modality, using a Unitherm Model 2022, in accordance with the ASTM E1530 [24].
Electrical resistivity measurements were carried out at room temperature with an Hewlett Packard 6516A Power Supply, equipped with an adjustable direct voltage generator in the range 0-3000 V; a three-electrode arrangement, equipped with a guard ring electrode, was used as test cell with a twofold aim: a) to get rid of surface leakage currents and b) to provide a uniform electric field distribution in the sample. For sensitivity purposes, measurements were performed by applying a constant DC voltage equal to 100 V, in the case of composites showing insulating behavior (i.e., base matrix), and equal to 5V, in the case of compounds

showing a conductive behavior (i.e., compounds containing MWCNT). A HP4140B picoammeter with resolution of 10^{-15} A was used to measure the current intensity. All reported values were taken after 2 minutes from the application of the DC voltage, when transient phenomena could be considered as extinguished and a steady state was reached.
Relative permittivity (ε) and loss factor (tg δ) were measured in the frequency range between 0.1 kHz and 10 MHz, at room temperature, by an impedance analyzer (HP 4192A) connected to a shielded 3-terminal measuring cell (Agilent 16451B Dielectric Text Fixture). The presence of a guard electrode at earth potentials, moreover, constraints the stray capacitances. The amplitude of the applied voltage was 1 V_{rms}.
For both electrical resistivity measurements and for dielectric spectroscopy, three specimen were used for each composite and the given values are an average of three measurements taken on each specimen.
Viscoelastic characterization of melts was performed using a parallel plate rheometer (ARES, TA Instruments, USA). Small amplitude oscillations, in the frequency range from 0.1 to 100 rad/s, were performed at 170, 190, 210 and 230 °C, using 25 mm parallel plates, under a dry nitrogen atmosphere to prevent thermal oxidation of the samples. Preliminary strain sweep tests were conducted in order to establish the linear viscoelastic region of studied formulations. Capillary rheological measurements were conducted, in a shear range of 100-10000 s^{-1}, at a temperature of 190°C, using CEAST SmartRheo (Instron ITW Test and Measurement Italia S.r.l.) with a capillary die of 1 mm diameter and a length of 30 mm. Entrance pressure drops were neglected while Mooney-Rabinowitsch correction for non-parabolic velocity profile was applied.
Morphological observations were performed using a field emission scanning electron microscope (model FEI QUANTA 200F). Cryo-fractured surfaces the samples were metalized with Au-Pd alloy before testing and micrographs were captured operating in high vacuum condition at voltage of 20 kV.

RESULTS AND DISCUSSION

Processability characteristics of hybrids were observed through torque and viscosity measurements. Indeed, while the first parameter represents the melt hindrance to processing-like deformation, the second one provides information about the melt resistance to simple shear flow. In Fig. 1(a), the mixing torque, measured during composite preparation, is reported as a function of the mixing time. From the beginning up to approximately 2 min, data show a non-monotonous trend corresponding to chamber filling, polymer densification, and melting. In the range between 2 and 7 min, as the mixing takes place and the system homogenizes, the torque reaches a steady-state level. As a consequence of the introduction of solid particle in molten polypropylene, the nanocomposites have a higher resistance to deformation with respect to the neat PP [25]. Interestingly, it should be noted that differences between ternary (PP/MWCNT/X) and binary (PP/MWCNT) formulations are very limited. The same considerations can also be derived from viscosity data plotted, in Fig. 1(b), against shear rate. At the temperature of 190°C, for all the systems, the viscosity is a decreasing function of the shear rate. It should be noted that composites show increased viscosities (and higher

relaxation times) with respect to the pure matrix as the presence of fillers restricts the polymer chain mobility due of the formation of a network; this behaviour is largely observed in literature [26]. At high shear rates, independently of the composition, all the composites curves do almost superimpose thus showing that the effects of both carbon nanotubes and secondary particles on the viscosity are very limited.

The data in Fig. 1 (a) and (b) lead to the conclusion that, even if a slight increase of torque and viscosity is detected in all compounds compared to the neat matrix, the overall processability of PP/MWCNT nanocomposites is almost unaffected by the introduction of the additional particles and by their size and shape.

Thermal properties, as evaluated from calorimetric analysis, are reported in Table 2 for all the investigated materials. In this regard, data from the second heating runs indicate that the addition of the secondary filler does not significantly affect neither the melting temperature nor the degree of crystallinity of PP that remain approximately equal to 168°C and 40%, respectively.

In Fig. 2 (a) thermal conductivity (κ) values of binary systems (PP/MWCNT) and ternary formulations (PP/MWCNT/X) are compared. In the binary system, the thermal conductivity of the neat PP (κ=0.093 $Wm^{-1}K^{-1}$) is positively influenced by the inclusion of carbon nanotubes resulting in an increase approximately equal to + 72%; moreover, the thermal conductivity of ternary formulations shows further improvements. Not surprisingly, the higher thermal conductivity (κ=0.246 $Wm^{-1}K^{-1}$), corresponding to +165% with respect to PP, is reached by hybrids containing BN due probably to its intrinsic higher thermal transport ability, compared to the other secondary particles considered so far (see Table 1). Lower improvements amounting at about +140%, +130% and +100% are verified for ternary compounds involving talc, ZnO and $CaCO_3$ as secondary fillers, respectively. In this case, contrary to the expectation, despite the intrinsic thermal properties of raw powders, talc appears to be the most effective filler probably thanks to its ability to build up conductive networks, as confirmed also by electrical measurements shown later. This effect can be due to a positive combination among mutual dispersion, packing factor and physical interactions between the two fillers.

Fig. 2(b) shows a comparison among the electrical resistivity (ρ_v) for the different compounds: hybrid formulations, bynary systems, and neat processed PP.

Results display an electrical resistivity for polypropylene matrix in the order of 10^{13} ohm*m, confirming its electrical insulating nature. The inclusion of 1.5 vol. % MWCNTs significantly reduces the resistivity at values of the order of 10^6 ohm*m and this reduction is further enhanced by the addition of 10 vol. % of micro-sized talc or $CaCO_3$ particles. This result is consistent with data from literature [27], where this behavior was attributed to the expected influence of inert particulate fillers on the dispersion of CNTs. The inclusion of $CaCO_3$ particles, by reducing the volume available for carbon nanotubes disposition, allows connections and facilitates movements of electrons through composites. On the contrary, both for sub-microsized BN (ρ_v~$2\cdot10^{11}$ ohm*m) or ZnO (ρ_v~$5\cdot10^{11}$ ohm*m) compounds, the volume resistivity decreases with respect to the neat PP, but remains higher with respect to detected values for the case of talc or $CaCO_3$. This high ρ_v values allow to exclude the formation of electrical conducting trackways that bridge the electrodes and suggest a good dispersion between fillers, as also confirmed in SEM images. In short, we can affirm that data in Fig. 2(b)

suggest that the electric paths promoted by carbon nanotubes are, in the presence of a second filler, affected by the mutual distribution of the fillers.

The dissipation factors (tg δ) of all investigated materials are reported as a function of the frequency in Fig. 3a. The dissipation factor takes into account different types of losses in an insulating material, usually attributed to conduction (Joule losses) and/or dielectric hysteresis phenomena (losses due to the movement of dipoles), which can occur in different ranges of frequencies. In our case, while the neat PP shows a dissipation factor almost frequency independent, the carbon-based formulations display a non-monotonous behavior with maxima in the frequency range of 0.1÷1 kHz. The dissipation factor increases by decreasing the size of secondary particles, according to the following sequence: tg $\delta(CaCO_3)$ < tg δ(Talc) < tg δ(BN) < tg δ(ZnO); the maximum value is obtained for PP/MWCNT composites.

For a better understanding of the phenomena, we have also plotted in Fig. 3.b the real part of the complex conductivity vs. frequency (i.e. the ac conductivity σ_{ac}). All systems show a conductivity value which is at least 3 orders of magnitude higher than that of the neat PP (which indeed couldn't be measured since it is lower than the resolution 10^{-12} S/m of the measuring instrument). For each composition there exists a critical frequency f_c above which the ac conductivity increases according to a typical power law [28]:

$$\sigma_{ac} = \sigma_0 f_c^s \qquad (2)$$

where s is a characteristic exponent close to unity. Above this value, the conduction losses become negligible.

It is interesting to observe that also the critical frequency depends on the size of the secondary particles: it is greater for smaller size secondary inclusions.

The peak in tg δ is found in the same frequencies range at which a polarization mechanism gradually fades. According to the Maxwell-Wagner model this behavior can be attributed to interfacial polarization phenomena, which are typical in composites. In this latter case, also a remarkable increase of relative dielectric constant with respect to the hosting matrix is recorded, as confirmed in Fig. 4.

In general, the permittivity (ε_r), similarly to the dissipation factor, is the result of different polarization phenomena (dipolar, interfacial, atomic), visible in specific frequency ranges. In this frame, the so-called interfacial polarization, restricted in the frequency range from 0.5 to 10 kHz, is attributed to the accumulation of space charges near filler-polymer and filler-filler interfaces and to the consequent orientation of electric dipoles along the direction of the applied field.

In particular, while no relaxation phenomena are observed for neat PP, being the permittivity independent of frequency for all the investigated hybrids, the permittivity sensibly increases in presence of fillers. For instance in the case of PP/MWCNT the relative permittivity is about 5.75 in the whole frequency range. The phenomenon is remarkable since the composite system is above the percolation threshold and the MWCNT agglomerates can form a micro-capacitor network that increases the stored energy [29]. With the addition of a secondary filler, the increase in ε_r is much higher and follows again the same trend observed for the dissipation factor tgδ in the overall investigated frequency range: $\varepsilon_r(CaCO_3)$ < ε_r(Talc) < ε_r(BN) <

ε_r(ZnO). In a few words, the relative permittivity is higher as the size of the secondary particle decreases.

As the frequency increases, the contribution to polarization of the different fillers decreases, due to the difficulty of the dipolar groups in following the variations of the applied field, and, as a consequence, the relative permittivity starts to decrease at f_1~ 400 Hz. The addition of the second filler produces also a second relaxation phenomenon clearly distinguishable at higher frequencies. In particular, the further decrease in permittivity starts at f_2~ 700 kHz in ZnO composites, which are the hybrid systems characterized by a second filler with the smallest size. The inception of the phenomenon occurs at higher frequencies as the filler size increases, probably because the smallest particles form larger dipolar groups that find much more difficult in orienting at the same pace as the electric field.

This consideration can be assumed as an indication of the mutual distribution of the two combined fillers in the resin. In principle, the introduction of a secondary filler, influencing the dispersion of the primary one, can lead to an increase of interfaces, inversely proportional to the state of their agglomeration in the composite. In general, the usual attitude of included particles to segregate may reduce the points of accumulation and orientation of dipoles with consequent reduction of the relative permittivity.

An indirect assessment of the mutual dispersion of included fillers can be drawn from dynamic-rheological measurements. It should be noted that small amplitude oscillatory tests are useful to gain information about the presence of structures under quasi-static conditions; these conditions are very different from capillary flow that, on the contrary, can destroy structures formed at rest.

In order to investigate how carbon nanotubes affect the melt rheological behaviour of compounds when combined with additional fillers, a comparison between storage moduli of ternary (PP/MWCNT/X) and binary systems (PP/X) was considered. In this regard, in Fig. 6, the viscoelastic behavior of investigated materials is reported in terms of storage modulus (G') curves as a function of the oscillatory frequency (ω).

In details, at low frequencies, all ternary formulations (PP/MWCNT/X) exhibit a solid-like behavior with orders-of-magnitude increases with respect to pure PP and a very weak dependency of viscoelastic functions on the frequency. This behavior can be related to the formation of interconnected structures, due principally to filler-matrix interactions, characterized by slow relaxation dynamics of the stresses. At high frequencies, G' curves tend to converge and to superimpose on pure PP behavior, thus showing a negligible contribution of the filler to fast relaxation dynamics.

It is clear that the presence of carbon nanotubes significantly changes the melt behaviour of binary systems (PP/X) in a way that depends on nature and dimension of secondary particles. In details, at a frequency of 0.1 rad/s, the storage modulus of binary systems containing $CaCO_3$ (particle size < 30 μm), approximately equal to 20 Pa, is drastically improved by the inclusion of MWCNTs, becoming in the range of 10^4 Pa. More limited, but still evident, increases of the same viscoelastic parameter are detected in the case of BN (particle size < 1 μm) and talc (particle size < 10 μm) where, at low frequencies, the storage modulus of ternary compounds is, respectively, one and two order of magnitude higher than of the corresponding binary formulation. In the case of ZnO (particle size < 100 nm), no substantial variation is observed

with the addition of MWCNT. The observed behaviours suggest that the inclusion of nanofillers (MWCNT) in a microcomposite systems may favour mutual filler packing and, consequently, the interactions among particles.

Further insights about mutual interactions may be gained by analysing more in details the rheological behaviour of investigated PP-based materials. In general, when carbon nanotubes are included in a polymer melt, three kind of interactions (polymer-polymer, filler-filler and polymer-filler) can occur and the influence of temperature on viscoelastic properties can provide further details especially on the polymer-polymer and polymer-filler networks [30]. In this regard, rheological data were collected at four different temperatures, 170, 190 and 210, and 230°C on binary (PP/X) and ternary formulations (PP/MWCNT/X) and the results are shown in Fig.6 in terms of loss tangent (Tan δ) vs. angular frequency.

It is evident that, for ternary formulations containing talc or $CaCO_3$, Tan δ curves at the different temperatures, roughly overlap, while, on the contrary, differences are visible for the systems containing BN or ZnO particles. This behaviour leads us to assume that for hybrids containing large-size secondary particles (talc and $CaCO_3$), the interaction between fillers are dominant and give rise to percolating-network structures that are temperature-independent. In the case of secondary particles with smaller sizes (ZnO and BN), connections between the filler particles take place through the polymeric chains of the hosting matrix and the percolated structure is constituted by entangled polymer-filler network. In this last case the rheological response of the system is clearly more temperature dependent.

Morphological observations support the above considerations about the fillers distribution. The reported SEM micrographs of hybrids have different magnification in order to highlight the different size of the secondary particles. In Fig. 8, some carbon nanotubes and additional particles are highlighted through dashed circles and continuous arrows, respectively. For hybrid systems containing $CaCO_3$ (see Fig. 8(a)), a poor mutual dispersion is observed with MWCNT agglomerates sharply separated from $CaCO_3$ particles. For the hybrids involving talc and MWCNT (see Fig. 8(b)) an apparently good dispersion of both fillers in matrix is visible. Indeed MWCNTs seem to be quite isolate, while talc lamellae appear distributed as to imply a possible mutual interaction. For systems containing BN and MWCNT (see Fig. 8(c)) an apparent good dispersion of both fillers is achieved with quite isolate (or small aggregates of) MWCNTs dispersed between platelets of BN. Also in the case of composites containing ZnO and MWCNTs, a homogeneous distribution of both fillers seems to be verified (Fig. 8(d)).

Finally, the above discussed thermal and electrical results can be summarized in a combined plot comparing thermal and electrical conductivities of all studied materials (Fig.9).

Taking the neat matrix and the PP/MWCNT as references, it is clear that the presence of electrically inert additional filler determinates always an increase in thermal conductivity but affects in opposite way the dielectric properties of ternary formulations due to the ability of the secondary filler to interrupt the electrical conductive network formed by the nanotubes. In particular, for hybrid composites containing the smaller BN or ZnO particles the final compounds possess enhanced thermal conductivity and low electrical conductivity. On the contrary hybrids containing $CaCO_3$ or Talc, even if a higher thermal conductivity is achieved the electrical conductive network of carbon nanotubes is not hindered and electrical conductivity remains almost equal to that of PP/MWCNT.

CONCLUSION

Binary and hybrid ternary systems based on polypropylene, filled with MWCNT alone or together with additional electrically inert particles, were prepared by melt compounding and characterized in terms of thermal and electrical properties. Sub-micronic pseudo-spherical zinc oxide (ZnO) and hexagonal boron nitride (BN), micronic lamellar talc and cubic calcium carbonate ($CaCO_3$) were used as secondary fillers for verifying their effect on thermal and dielectric properties of carbon-based composites.

The results—supported by dynamic rheological measurements and scanning electron microscopy observations—are discussed in terms of mutual dispersion of fillers and show that:

i) improvements of the thermal conductivity of hybrids are achieved without compromising the processability of the composites;

ii) the target of developing thermally conductive and electrical insulating can be met combining fillers with different shape but similar in size (in our case MWCNTs + ZnO particles and MWCNTs + BN particles) that, therefore, able to ensure appropriate packing and interactions;

iii) an upgrade of both thermal and electrical conduction is observed in hybrids obtained with the addition of micrometric electrically inert particles (as $CaCO_3$ or Talc).

REFERENCES

[1] Ashby, M. F.; Brechet, Y. J. M. *Acta Mater* 2003, *51*, 5801–5821.

[2] Leong, Y.W.; Ishak, Z.A. Mohd.; Ariffin, A. J. Appl. Polym. Sci. 2004, 91, 3327-3336

[3] Salkhord, S.; Sadeghi Ghari, H. J. Appl. Polym. Sci 2015, 132, 42744-42756

[4] Luan, B. C. D.; Huang, J.; Zhang, J. J. Appl. Polym. Sci. 2015, 132, 42302-42309

[5] Lee, G.W.; Park, M.; Kim, J.; Lee, J. I.; Yoon, H. G. Compos Part A 2006, 37, 727-734.

[6] Pak, S. Y.; Kim, H. M.; Kim, S. Y.; Youn, J. R. Carbon 2012, 50, 4830–4838.

[7] Palza, H.; Garzón, C.; Arias, O. eXPRESS Polym Lett 2012, 6, 639-46.

[8] Tsekmes, I. A.; Morshuis, P. H. F.; Smit, J. J.; Kochetov, R. IEEE Electr Insul Mag 2015, 31, 32-42.

[9] Dang, T. M. L.; Kim, C-Y; Zhang, Y.; Yang, J-F.; Masaki, T. Compos Part B 2017, 114, 237-246.

[10] Choi, S.; Kim, J. Compos Part B 2013, 51,140-147.

[11] Srinivas, K.; Bhagyashekar, M. S. Journal of Minerals and Materials Characterization and Engineering 2015, 3, 76-84.

[12] Yuan, Y. F.; Zhang, H. B.; Li, X.; Li, X. Z.; Yu, Z. Z. Compos Part A 2013, 53, 137-144.

[13] Mahanta, N. K.; Loos, M. R.; Zlocozawer, I. M. J Mater Res 2015, 30, 959-966.

[14] Zhidong, H.; Fina, A. Prog Poly Sci 2011;36, 914-944.

[15] Patti, A.; Russo, P.; Acierno, D.; Acierno, S. Compos Part B 2016, 94, 350-359.

[16] Ng, H.Y.; Lu, X.; Lau, S. K. Polym Comp 2005, 26, 66-73.

[17] Weidenfeller, B.; Hofer, M.; Schilling, F. R. Compos Part A 2004, 35, 423-429.

[18] Cheewawuttipong, W.; Fuoka, D.; Tanoue, S.; Uematsu, H.; Iemoto, Y. Energ Procedia 2013, 34, 808-817.
[19] Zhang, L. M.; Dai, G. C. eXPRESS Polym Lett 2007, 1, 608-615.
[20] Huang, X.; Jiang, P.; Tanaka, T. IEEE Electr Insul Mag 2011; 27, 8-16.
[21] Ebadi-Dehaghani, H.; Reiszadeh, M.; Chavoshi, A.; Nazempour, M.; Vakili, M. J Macromol Sc Part B Phys 2014, 53, 93-107.
[22] Ahrens, T.J. Rock physics and phase relations: A handbook of physical constant. American Geophysical Union Reference: Washington, 1995; p.236.
[23] Brandrup J and Immergut EH. Polymer Handbook. John Wiley & Sons: New York,1989; p.1850.
[24] ASTM E1530-99, Standard Test Method for Evaluating the Resistance to Thermal Transmission of Materials by the Guarded Heat Flow Meter Technique.
[25] Al-Saleh, M. H. Synth Met 2015, 209, 41-46.
[26] Di Maio, L.; Garofalo, E.; Scarfato, P.; Incarnato, L. Polym Compos 2015, 36, 1135-1144.
[27] Bao, H. D.; Guo, Z. X.; Yu, J. Polymer 2008, 49, 3826–3831.
[28] Barrau, S.; Demont, P.; Peigney, A.; Laurent, C.; Lacabanne, C.; Macromolecules 2003, 36, 5167-5194.
[29] Musto, P.; Russo, P.; Cimino, F.; Acierno, D.; Lupò, G.; Petrarca, C. Eur Polym J 2015; 64, 170-178.
[30] Potschke, P.; Abdel-goad, M.; Alig, I.; Dudkin, S.; Lellinger, D. Polymer 2004, 45, 8863-8870.

FIGURE 1 (a) Torque vs mixing time as measured during the preparation of the composites at 190°C; (b) viscosity vs shear rate as measured in capillary rheometer at 190°C (legend as in Fig. 1(a))

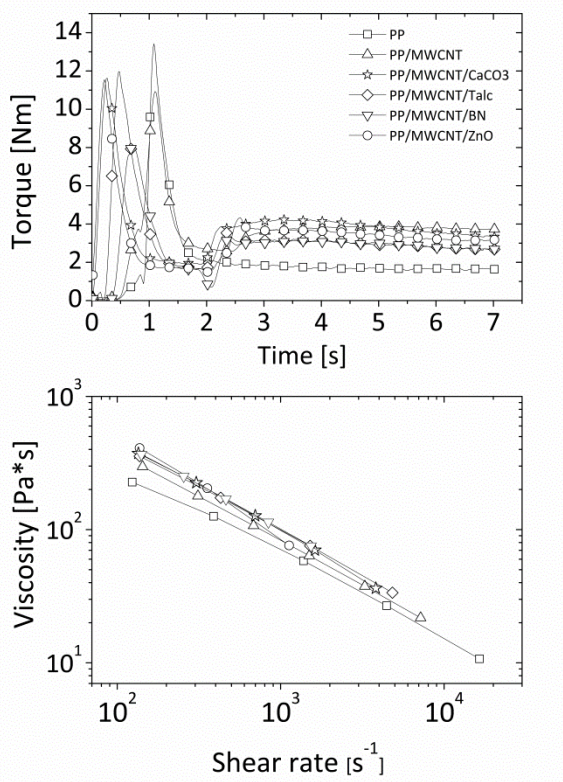

FIGURE 2 Thermal conductivity (a) and electrical conductivity (b) of investigated hybrid materials (legend as in Fig.2(a))

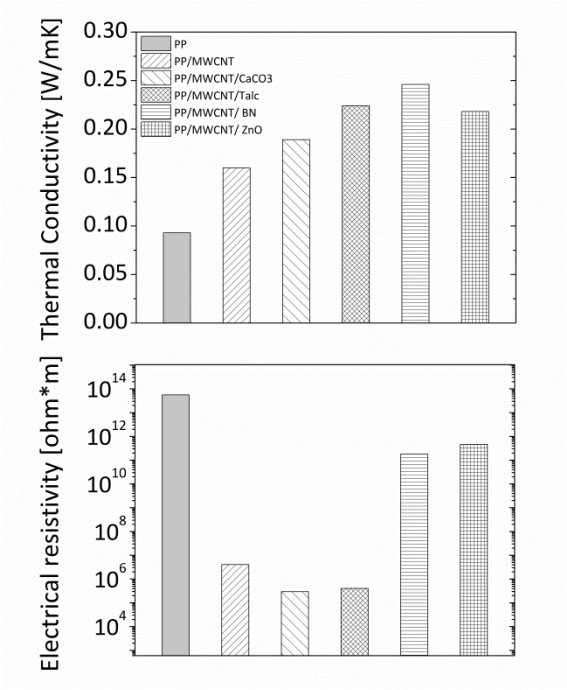

FIGURE 3 Comparison among dissipation factors of ternary formulations

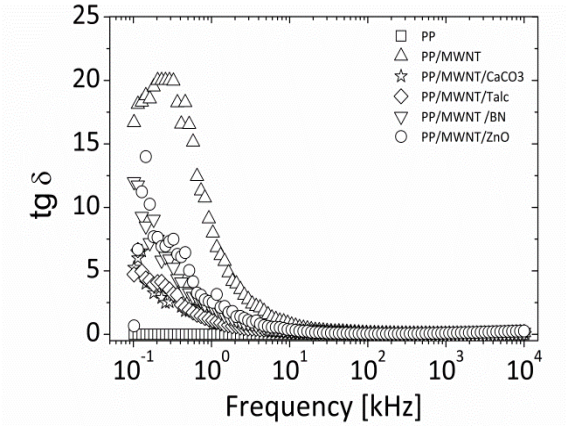

FIGURE 4 Comparison among permittivity (ε) of investigated systems

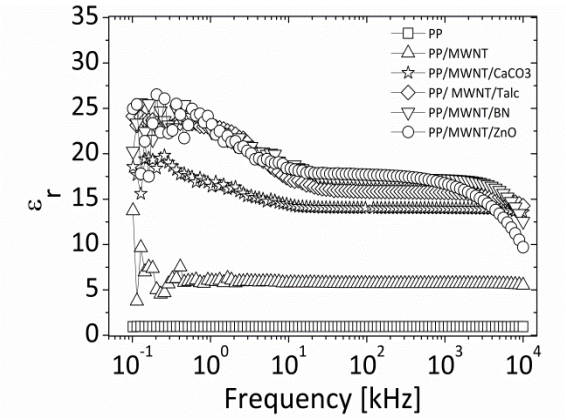

FIGURE 5 **(**Inserire didascalia)scegliere la figura più leggibile tra le due

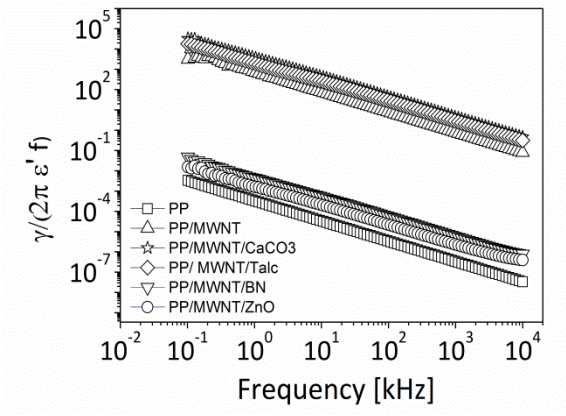

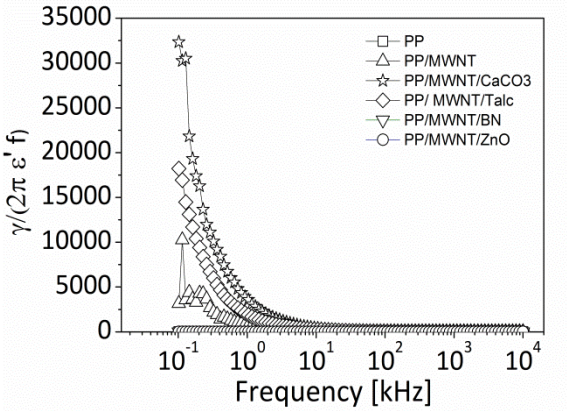

FIGURE 6 Comparison among storage modulus as a function of frequency for binary and ternary compounds at a temperature of 190 °C

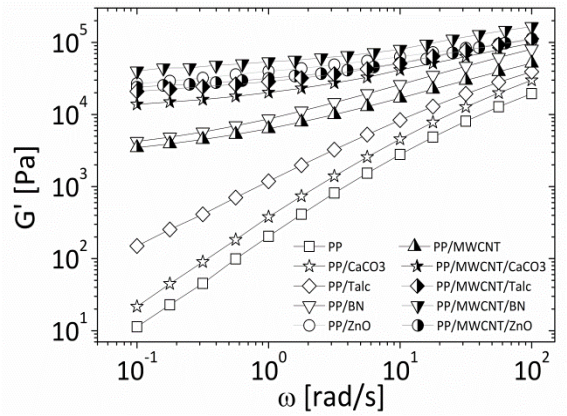

FIGURE 7 Comparison between dissipation factors of hybrid materials and their respective binary systems without MWCNT, at a temperature of 170, 190, 210, 230°C, for different particles:(a) CaCO3; (b) Talc; (c) BN; (d) ZnO

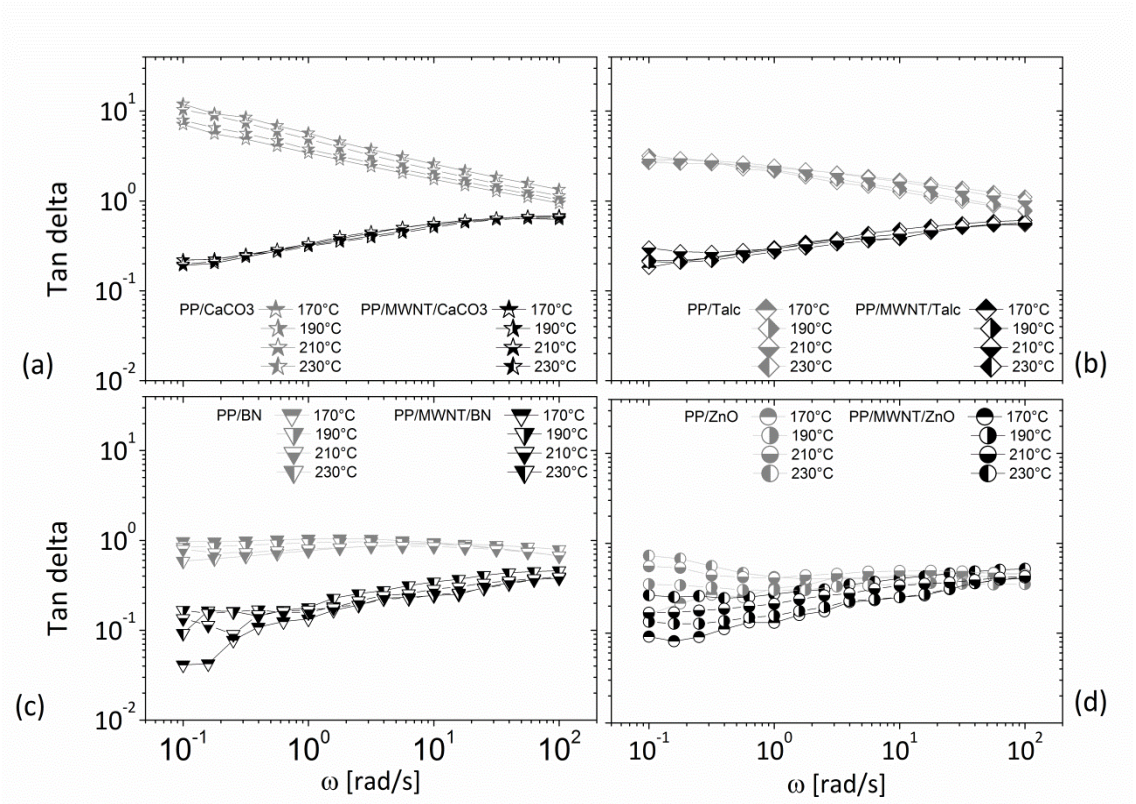

FIGURE 8 SEM micrographs of hybrid systems: (a) PP/MWCNT/CaCO3; (b) PP/MWCNT/Talc; (c) PP/MWCNT/BN; (d) PP/MWCNT/ZnO. Specific points, related to carbon nanotubes and secondary filler, are underlined through dashed circles and continuous arrows, respectively

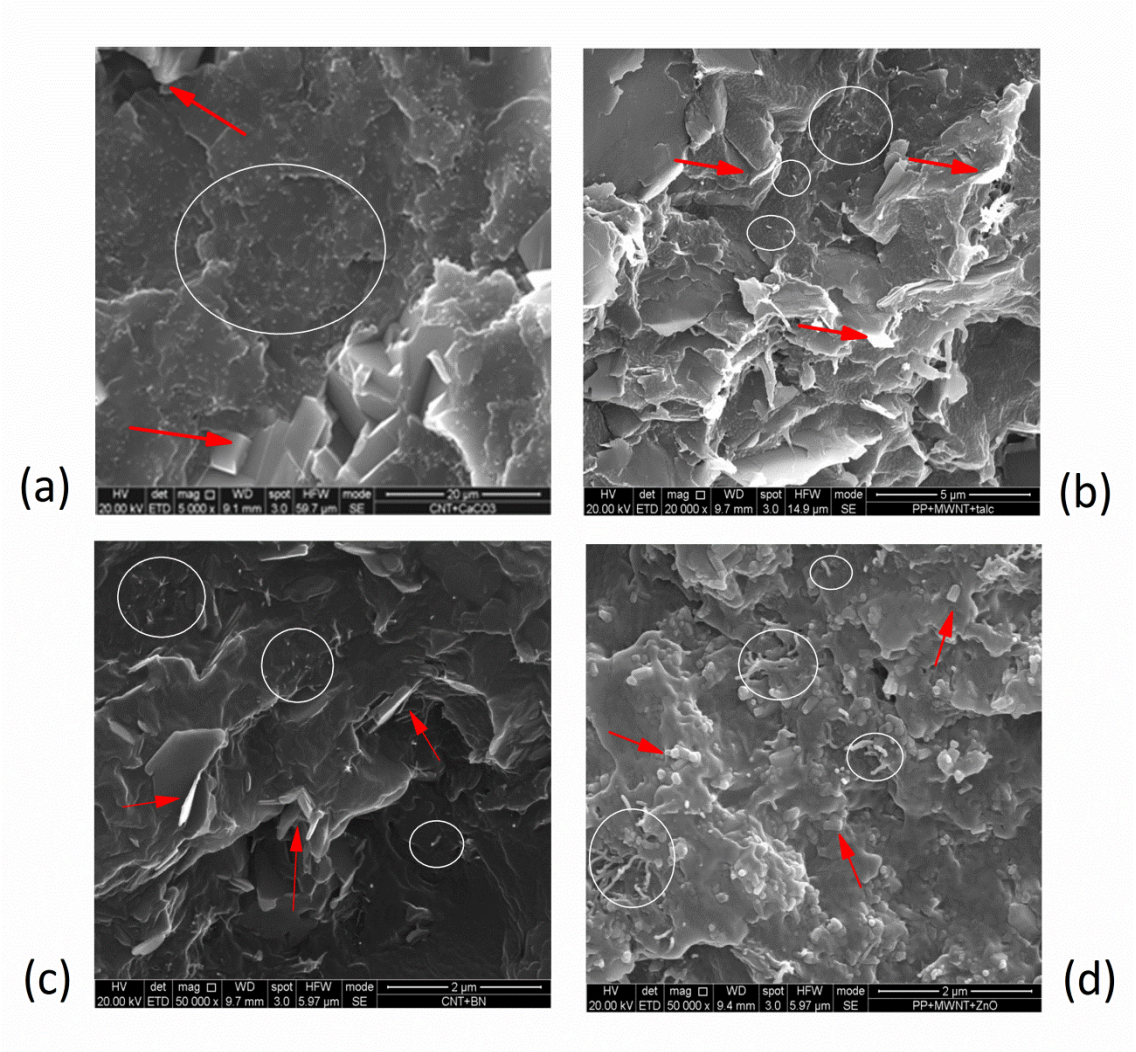

FIGURE 9 Thermal conductivities vs electrical ones for analyzed materials.

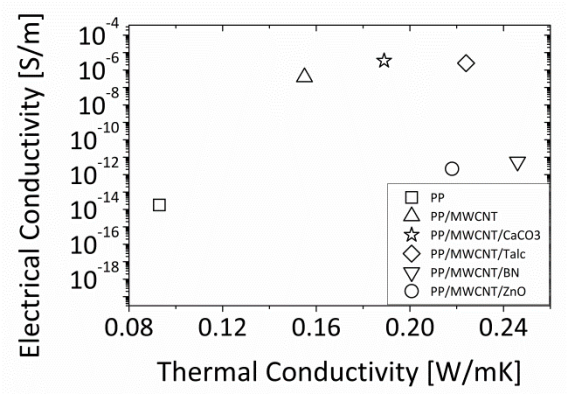

TABLE 1 Properties of secondary filler particles.

Filler	**Shape**	**Average size [μm]**	**Density [g/cm^3]**	**Thermal Conductivity [W/mK]**	**Electrical resistivity [ohm*cm]**
$CaCO_3$	Cubic	30	2.71	4.5 [20]	10^{14}
Talc	Lamellar	10	2.78	⊥1.76 // 10.69 [22]	$>10^9$
BN	Hexagonal platelets	1	2.93	⊥2 // 400 [14]	10^{13}
ZnO	Pseudo-spherical	0.1	5.61	60 [14]	$>10^8$

TABLE 2 Melting properties of hybrid materials as obtained by DSC experiments

Materials	**T_m [°C]**	**ΔH_c [J/g]**	**X_c [%]**
PP	166	86.2	41
PP/MWCNT	167	82.9	41
PP/MWCNT/$CaCO_3$	169	61.9	41
PP/MWCNT/Talc	168	62.2	41
PP/MWCNT/BN	169	47.9	39
PP/MWCNT/ZnO	168	62.1	40

GRAPHICAL ABSTRACT